

SPHERICAL HARMONICS FINITE ELEMENT SOLUTION OF THE LEAST-SQUARES NEUTRON TRANSPORT EQUATION

E. Varin and G. Samba
Commissariat à l'Énergie Atomique, DIF,
BP 12, 91680 Bruyères-Le-Châtel, France
gerald.samba@cea.fr

and R. Roy
Ecole Polytechnique de Montréal, IGN,
P.O. Box 6079, Station Centre-Ville, Montréal H3C 3A7, Canada
elisabeth.varin@polymtl.ca, robert.roy@polymtl.ca

ABSTRACT

To solve the neutron Boltzmann equation in anisotropic or void regions, one may use deterministic methods such as the discrete ordinates method or the even-parity approach. Both methods have shown numerous applications and developments in the last 30 years. Nevertheless both exhibit drawbacks in three-dimensions void regions that require special treatments, such as using characteristics method or first order spherical harmonic method. The basic idea of the work presented here is to define a unique approach that can be use in 3D void regions without any special care. The least-squares technique is applied to the neutron transport equation. Combined with a spherical harmonic expansion of the angular flux, this approach leads to a variational formulation suitable for continuous finite elements. Extensions are proposed to allow for the 3D transport in void regions and complete derivation of discrete equations is given for anisotropic media. Numerical results show that ARTEMIS, a transport solver based on this method, gives solutions free of ray effects. These results include 3D tests on the Kobayashi first benchmark problem.

1. INTRODUCTION

In radiation transport problems, as shielding applications, the solution of the Boltzmann transport equation is generally obtained either by the discrete ordinates deterministic method or by the R_N even-parity method. The discrete ordinates or S_N method is based on the determination of the angular neutron flux along specific traveling directions, usually points of Gaussian quadrature. The domain is divided into cells, and the space variable is discretized using finite difference approaches.^[1] In realistic radiation problems, where sources are spatially localized, irradiating in a large media with low interactions, the S_N method shows ray-effect problems, which require a finer angular quadrature. In medical applications for example, the source can be so narrowed that a specific angular quadrature has to be elaborated to follow the neutron transport. Moreover, the finite difference scheme to discretize the spatial variables

requires an explicit sweep of the geometry, which can become intractable or even impossible to define in three dimensions.^[2]

To eliminate ray effects and use finite element method, another approach is the even-parity transport formulation where the angular neutron flux is developed into spherical harmonics. The flux moments are obtained as the solution of P_N equations.^[3] Standard P_N approaches propose to substitute odd moments (l odd) into even equations, resulting in systems of diffusion-like equations.^[3-5] This process is also equivalent to defining a variational functional^[6] on the even-parity transport equation. However, the diffusion-like coefficients imply the inversion of total cross sections ($1/\sigma$), introducing singularity for void regions.

This paper extends a least-squares technique, originally developed by K.J Ressel^[7], in the general context of a full 3D transport solver called ARTEMIS.^[8] The ARTEMIS solver respects the diffusive limits, but it can also treat void regions.^[8] In the first section, the P_N discretization of the neutron equation is described in 3D Cartesian domains with respect to anisotropic and multiplicative media. The least squares approach is developed in the second section as well as the finite element integration. In Section 3, the introduction of boundary conditions into the resulting linear system is explained for both reflective and fixed incoming flux conditions. Numerical results are then proposed in the last section for the extension to multigroup anisotropic regions and for a realistic 3D void problems. Finally, some conclusions are drawn and on-going research is sketched.

2. SPHERICAL HARMONICS APPROXIMATION IN 3D CARTESIAN GEOMETRIES

In an isotropic media \mathfrak{R} , the one-speed steady-state neutron equation is given by:

$$\vec{\Omega} \cdot \vec{\nabla} \psi(\vec{r}, \vec{\Omega}) + \sigma(\vec{r}) \psi(\vec{r}, \vec{\Omega}) = \sigma_s(\vec{r}) P \psi(\vec{r}, \vec{\Omega}) + q(\vec{r}, \vec{\Omega}) \quad (1)$$

where σ is the total cross section, σ_s the scattering kernel and q an external neutron source. The projector operator P is defined as

$$P \psi(\vec{r}, \vec{\Omega}) = \int_{4\pi} d^2\Omega' \psi(\vec{r}, \vec{\Omega}')$$

The incoming flux conditions on boundary $\Gamma = \Gamma_1 \cap \Gamma_2$ are:

$$\begin{cases} \psi(\vec{r}, \vec{\Omega}) = h(\vec{r}, \vec{\Omega}) & \text{for } \vec{n} \cdot \vec{\Omega} < 0, \quad \vec{r} \in \Gamma_1 \\ \psi(\vec{r}, \vec{\Omega}_1) = \psi(\vec{r}, \vec{\Omega}_2) & \text{for } \vec{n} \cdot \vec{\Omega}_1 < 0, \quad \vec{\Omega}_2 = \vec{\Omega}_1 - 2(\vec{n} \cdot \vec{\Omega}_1)\vec{n}, \quad \vec{r} \in \Gamma_2 \end{cases} \quad (2)$$

where $\psi(\vec{r}, \vec{\Omega})$ is the angular neutron flux, fixed on Γ_1 and reflected on Γ_2 . The solution to equation (1) is obtained numerically after discretizations of the angular ($\vec{\Omega}$) and spatial (\vec{r}) variables. To maintain a result free of ray effects in three dimensions, the P_N approximation is chosen for the angular variable discretization. The flux is developed on a spherical harmonics basis as:

$$\psi(\vec{r}, \vec{\Omega}) = \sum_{l=0}^{\infty} \sum_{m=-l}^l \phi_{lm}(\vec{r}) Y_l^m(\vec{\Omega}) \quad (3)$$

$$\text{with } \phi_{lm}(\vec{r}) = \int_{4\pi} d^2\Omega' Y_l^{m*}(\vec{\Omega}') \psi(\vec{r}, \vec{\Omega}') \quad (4)$$

where Y_l^{m*} is the conjugate of Y_l^m , and ϕ_{lm} are called the flux moments. For an angular direction $\vec{\Omega} = (\varphi, \theta)$, with $\mu = \cos \theta$, the harmonics are defined in complex arithmetics by:

$$Y_l^m(\vec{\Omega}) = (-1)^m C_{l,m} P_l^m(\mu) e^{im\varphi} \quad (5)$$

where $P_l^m(\mu)$ are the associated Legendre polynomials and $C_{l,m}$ is chosen so that the basis is orthonormal as:

$$\int_{4\pi} d^2\Omega' Y_l^{m*}(\vec{\Omega}') Y_{l'}^{m'}(\vec{\Omega}') = \delta_{ll'} \delta_{mm'} \quad (6)$$

The flux expansion (3) is exact but it implies an infinite development. In the R_N approximation, we truncate the series and define that the flux moments $\phi_{lm}(\vec{r}) = 0$ for $l > N + 1$, that is the summation is limited to $l = N$. It is clear that when N tends to infinity, the angular flux is exact.

Prior to substitute the flux expansion (3) into the transport equation (1), the unknowns are ordered using a vector notation:

$$\psi = \vec{Y}^T \vec{\phi}(\vec{r}) \quad (7)$$

where $\vec{Y}^T = \{Y_0^0, Y_1^{-1}, Y_1^0, Y_1^1, \dots, Y_l^{-m}, \dots, Y_l^m, \dots\}^T$ and $\vec{\phi}^T = \{\phi_{00}, \phi_{1,-1}, \dots, \phi_{lm}, \dots\}^T$.

In 3D Cartesian geometries, the transport equation with the flux expression (7) is:

$$\Omega_x \frac{\partial}{\partial x} \vec{Y}^T \vec{\phi} + \Omega_y \frac{\partial}{\partial y} \vec{Y}^T \vec{\phi} + \Omega_z \frac{\partial}{\partial z} \vec{Y}^T \vec{\phi} + \sigma \vec{Y}^T \vec{\phi} - \sigma_s P \vec{Y}^T \vec{\phi} = q \quad (8)$$

where the unknowns are the $(N + 1)^2$ flux moments $\vec{\phi}$.

The streaming terms $\Omega_x Y_l^m$, $\Omega_y Y_l^m$ and $\Omega_z Y_l^m$ are developed using recurrence relations for the Legendre polynomials. They results in linear combinations of harmonics $Y_{l\pm 1}^{m\pm 1}$ in X and Y directions and of harmonics $Y_{l\pm 1}^m$ in Z directions. In matrix form, they are written as:

$$\begin{cases} \Omega_x \vec{Y}^T \frac{\partial}{\partial x} \vec{\phi} = \vec{Y}^T \mathbf{D}_x \frac{\partial}{\partial x} \vec{\phi} \\ \Omega_y \vec{Y}^T \frac{\partial}{\partial y} \vec{\phi} = i \vec{Y}^T \mathbf{D}_y \frac{\partial}{\partial y} \vec{\phi} \\ \Omega_z \vec{Y}^T \frac{\partial}{\partial z} \vec{\phi} = \vec{Y}^T \mathbf{D}_z \frac{\partial}{\partial z} \vec{\phi} \end{cases} \quad (9)$$

where \mathbf{D}_x , \mathbf{D}_y and \mathbf{D}_z are sparse matrices containing the spherical harmonics coupling coefficients.

To obtain $(N + 1)^2$ equations for the flux moments, equation (8) is multiplied by every Y_l^{m*} , $l < N + 1$ and then integrated over all angular directions. It results into a system of equations, which can be written in matrix form as:

$$P \vec{Y}^* \vec{Y}^T [\mathbf{D}_x \frac{\partial}{\partial x} \vec{\phi} + i \mathbf{D}_y \frac{\partial}{\partial y} \vec{\phi} + \mathbf{D}_z \frac{\partial}{\partial z} \vec{\phi}] + P \vec{Y}^* \sigma \vec{Y}^T \vec{\phi} - P \vec{Y}^* \sigma_s P \vec{Y}^T \vec{\phi} = P \vec{Y}^* q \quad (10)$$

The orthonormalization of the harmonics (6) produces that:

$$P \vec{Y}^* \vec{Y}^T = I \quad (\text{the identity matrix})$$

Moreover, because the first harmonics Y_0^0 is exactly 1, and with the definition of matrix $\underline{\delta}^0$, $\{\underline{\delta}^0\}_{l,k} = \delta_{l1} \delta_{k1}$, the projector P applied to the flux gives:

$$P \vec{Y}^T \vec{\phi}(\vec{r}) = \phi_{0,0} = \vec{Y}^T \underline{\delta}^0 \vec{\phi}$$

Similarly,

$$P \vec{Y}^* \sigma_s P \vec{Y}^T \vec{\phi} = \sigma_s \underline{\delta}^0 \vec{\phi}$$

Using these formulations, one obtains the flux moment equations in matrix form:

$$[\mathbf{D}_x \frac{\partial}{\partial x} \vec{\phi} + i\mathbf{D}_y \frac{\partial}{\partial y} \vec{\phi} + \mathbf{D}_z \frac{\partial}{\partial z} \vec{\phi}] + \mathbf{R}\vec{\phi} = \vec{Q} \quad (11)$$

where the matrix $\mathbf{R} = \sigma I - \sigma_s \underline{\delta}^0 = \sigma(I - \underline{\delta}^0) + \sigma_a \underline{\delta}^0$ and the vector $\vec{Q} = \{q_{l,m}\}^T$, $q_{l,m}$ are the source moments defined by

$$q_{l,m} = \int_{4\pi} d^2\Omega' Y_l^{m*}(\vec{\Omega}') q(\vec{r}, \vec{\Omega}')$$

2.1. TREATMENT OF BOUNDARY CONDITIONS

The flux expansion (3) is inserted into the boundary conditions (2). For 3D Cartesian geometries, the boundaries are planes perpendicular to the axis and these are easy to identify with respect to the angular variable (φ, θ) limits. We refer to the X boundaries as: the plane perpendicular to the X axis at the smallest x-ordinate is noted X_- and its symmetric plane at the largest x-ordinate is X_+ . The definition applies to Y and Z axis as well.

First, the reflective boundary conditions are derived. Because of the spherical harmonics definition, the reflexion of the incoming flux is replaced by $\frac{N(N+1)}{2}$ combination of flux moments as:

$$\begin{cases} X_{\pm} & \phi_{l,m} - \phi_{l,-m} = 0 & \forall l, m > 0, \vec{r} \in \Gamma_{2x} \\ Y_{\pm} & \phi_{l,m} - (-1)^m \phi_{l,-m} = 0 & \forall l, m > 0, \vec{r} \in \Gamma_{2y} \\ Z_{\pm} & \phi_l^m = 0 & l + m \text{ odd}, \vec{r} \in \Gamma_{2z} \end{cases} \quad (12)$$

Note that for Z_{\pm} , the well-known one-dimensional conditions when $m = 0$ are recovered.

Fixed flux boundary conditions can be introduced using the Marshak conditions^[9] This approximation consists on replacing $\psi(\vec{r}, \vec{\Omega}) = h(\vec{r}, \vec{\Omega})$ by an integral expression as:

$$\int_{\vec{n} \cdot \vec{\Omega} < 0} d^2\Omega' Y_l^{m'*}(\vec{\Omega}') \psi(\vec{r}, \vec{\Omega}') = \int_{\vec{n} \cdot \vec{\Omega} < 0} d^2\Omega' Y_l^{m'*}(\vec{\Omega}') h(\vec{r}, \vec{\Omega}') \quad (13)$$

$l' \text{ odd}, -l' \leq m \leq l'$

The integration across the perpendicular boundaries is done analytically, it results in $\frac{(N+1)(N+2)}{2}$ equations linking all flux moments.

These two types of boundary conditions are expressed in matrix form as:

$$\begin{cases} \mathbf{C}_1^T \vec{\phi} = \vec{d}, & \text{for } \vec{r} \in \Gamma_1 \\ \mathbf{C}_{2i}^T \vec{\phi} = 0, & \text{for } \vec{r} \in \Gamma_{2i}, i = x, y, z \end{cases} \quad (14)$$

where $\mathbf{C}_1(l, m, l', m') = \int d\varphi \int d\mu Y_l^{m'*}(\mu, \varphi) Y_l^m(\mu, \varphi)$ and the fixed value integrals $d(l, m) = \int d\varphi \int d\mu h Y_l^m(\mu, \varphi)$ and rows of \mathbf{C}_{2i} represent equation (12).

The isotropic transport equation (1) with its boundary conditions (2) has been discretized by R_N approximation into the system of equations (11) with boundary conditions (14).

2.2. EXTENSIONS FOR MULTIGROUP ANISOTROPY

One follows a similar approach to derive the anisotropic multigroup P_N equations. In anisotropic media the transport equation becomes:

$$\left[\vec{\Omega} \cdot \vec{\nabla} + \sigma(\vec{r}) \right] \psi(\vec{r}, \vec{\Omega}) = \int_{4\pi} d^2\Omega' \sigma_s(\vec{r}, \vec{\Omega} \cdot \vec{\Omega}') \psi(\vec{r}, \vec{\Omega}') + q(\vec{r}, \vec{\Omega}) \quad (15)$$

The scattering kernel σ_s is developed on the Legendre polynomial basis as:

$$\sigma_s(\vec{r}, \vec{\Omega} \cdot \vec{\Omega}') = \sum_{l=0}^{\infty} \frac{2l+1}{4\pi} \sigma_l(\vec{r}) P_l^0(\vec{\Omega} \cdot \vec{\Omega}') \quad (16)$$

where $\sigma_l(\vec{r})$ is the scattering cross section of anisotropy order l . When $l = 0$, σ_0 is the isotropic cross section. This infinite expansion is exact but usually limited to the order M based on the cross-section library data. The addition theorem of the spherical harmonics^[10] gives an expression for $P_l^0(\vec{\Omega} \cdot \vec{\Omega}')$ as a function of Y_l^m and Y_l^{m*} .

The scattering source becomes with both flux and scattering kernel expansions:

$$\begin{aligned} \int_{4\pi} d^2\Omega' \sigma_s(\vec{r}, \vec{\Omega} \cdot \vec{\Omega}') \psi(\vec{r}, \vec{\Omega}') &= \int_{4\pi} d^2\Omega' \sum_{l=0}^M \sigma_l(\vec{r}) \sum_{m=-l}^l Y_l^m(\vec{\Omega}) Y_l^{m*}(\vec{\Omega}') \psi(\vec{r}, \vec{\Omega}') \\ &= \sum_{l=0}^M \sigma_l(\vec{r}) \sum_{m=-l}^l Y_l^m(\vec{\Omega}) \phi_{lm}(\vec{r}) \end{aligned}$$

Replacing the scattering source into the transport equation (15) prior to multiply by all conjugate harmonics and to integrate over angular directions, one obtains the P_N anisotropic equations in matrix form:

$$\left[\mathbf{D}_x \frac{\partial}{\partial x} \vec{\phi} + i \mathbf{D}_y \frac{\partial}{\partial y} \vec{\phi} + \mathbf{D}_z \frac{\partial}{\partial z} \vec{\phi} \right] + \tilde{\mathbf{R}} \vec{\phi} = \vec{Q} \quad (17)$$

where $\tilde{\mathbf{R}} = \sigma I - \vec{\sigma}_s^T \underline{\underline{\delta}}^M$ with $\vec{\sigma}_s^T = \{\sigma_0, \sigma_1, \sigma_1, \sigma_1, \dots, \sigma_l, \dots, \sigma_M, 0, \dots, 0\}$ and $\{\underline{\underline{\delta}}^M\}_{kk} = 1, k < M + 1, = 0, k > M$.

In order to use the method for reactor physics applications, multigroup and multiplicative media are considered. There, the multigroup anisotropic transport equation is:

$$\begin{aligned} \vec{\Omega} \cdot \vec{\nabla} \psi^g(\vec{r}, \vec{\Omega}) + \sigma^g(\vec{r}) \psi^g(\vec{r}, \vec{\Omega}) - P \sigma_s^{gg}(\vec{r}, \vec{\Omega} \cdot \vec{\Omega}') \psi^g(\vec{r}, \vec{\Omega}') \\ = \sum_{g'=1, g' \neq g}^G P \sigma_s^{g' \rightarrow g}(\vec{r}, \vec{\Omega} \cdot \vec{\Omega}') \psi^{g'}(\vec{r}, \vec{\Omega}') \\ + \frac{1}{k} \chi^g \sum_{g'=1}^G \nu \sigma_{fg'}(\vec{r}) P \psi^{g'}(\vec{r}, \vec{\Omega}') \end{aligned} \quad (18)$$

where $\frac{1}{k}$ is the problem eigenvalue and $\nu \sigma_{fg'}$ is the fission cross section times the number of produced neutrons in the g' energy group and χ^g is the neutron energy spectra of group g .

Following the same procedure to develop the P_N equations, one obtains:

$$\left[\mathbf{D}_x \frac{\partial}{\partial x} + i \mathbf{D}_y \frac{\partial}{\partial y} + \mathbf{D}_z \frac{\partial}{\partial z} \right] \vec{\phi}^g + \tilde{\mathbf{R}}^g \vec{\phi}^g = \sum_{g'=1, g' \neq g}^G \mathbf{S}^{g'g} \vec{\phi}^{g'} + \frac{1}{k} \chi^g \sum_{g'=1}^G \mathbf{F}^{g'} \vec{\phi}^{g'} \quad (19)$$

where $\tilde{\mathbf{R}}^g$ is composed of σ^g and σ_l^{gg} , the diagonal matrix $\mathbf{S}^{g'g}$ is the group-to-group scattering matrix formed with $\sigma_l^{g'g}$ and the matrix $\mathbf{F}^{g'}$ is the fission matrix, as $\mathbf{F}^{g'} = \nu \sigma_{fg'}(\vec{r}) \underline{\delta}^0$.

In order to use continuous finite elements, one develops a symmetric variational functional, where no total cross section inversion is required. This functional is based on the least-squares approach developed by K.J. Ressel. [7,11]

3. LEAST-SQUARES APPROACH AND FINITE ELEMENT DISCRETIZATION

The least squares method is a general approach where the solution of an equation is replaced by a residual minimization technique. Here, the least-squares formulation of the isotropic one-speed neutron equation is:

- find $\psi \in V$ such that $\forall u \in V$:

$$\langle \mathcal{L}u, \mathcal{L}\psi \rangle = \langle \mathcal{L}u, q \rangle \quad (20)$$

where the functional \mathcal{L} by $\mathcal{L}\psi = \vec{\Omega} \cdot \vec{\nabla}\psi(\vec{r}, \vec{\Omega}) + \sigma(\vec{r})\psi(\vec{r}, \vec{\Omega}) - \sigma_s(\vec{r})P\psi(\vec{r}, \vec{\Omega})$ and where the scalar product is defined by

$$\langle u, v \rangle = \int_{\mathfrak{R}} d^3r' \int_{4\pi} d^2\Omega' u v^*$$

with v^* being the conjugate of v .

Manteuffel, Ressel and Starke^[11] have demonstrated that this problem has a unique solution in most domains providing a scaling operator be applied prior to the least-squares formulation. This scaling is required to maintain the bounds of continuity and V-ellipticity of the bilinear form $\langle \mathcal{L}\psi, \mathcal{L}\psi \rangle$ independent of the problem parameters σ and σ_s . This means that scaling is required to maintain the diffusion limit^[12] ($\sigma > 1$ mfp) when using a P_1 expansion and linear finite elements.^[7,8] No scaling is required in case of thin transport domain ($\sigma \leq 1$ mfp), which is the scope of the results presented later. The solution space V is approximated by a discrete space V_h , where every element is defined by:

$$v_h(\vec{r}, \vec{\Omega}) = \sum_{l=0}^N \sum_{m=-l}^l \phi_{lm}^h(\vec{r}) Y_l^m(\vec{\Omega}) \quad (21)$$

The angular flux is represented by the spherical harmonics P_N development as exposed in the previous section. One can show^[8] that the equation (20) is equivalent to the least squares formulation of the R_N equations with the definition (21) of v_h . The least-squares equation (20) becomes:

- find $\vec{\phi} \in V_h$ such that $\forall \vec{v}^h \in V_h$:

$$\int_{\mathfrak{R}} d^3r' (\mathbb{M}\vec{v}^h)^H \mathbb{M}\vec{\phi} = \int_{\mathfrak{R}} d^3r' (\mathbb{M}\vec{v}^h)^H \vec{Q} \quad (22)$$

where the index H denotes hermitian transformation and the discretized R_N transport functional is

$$\mathbb{M}\vec{\phi} = [\mathbf{D}_x \frac{\partial}{\partial x} \vec{\phi} + i\mathbf{D}_y \frac{\partial}{\partial y} \vec{\phi} + \mathbf{D}_z \frac{\partial}{\partial z} \vec{\phi}] + \mathbf{R}\vec{\phi}$$

A least squares approach is also used to consistently apply the boundary conditions (14), which means

that the boundary residual is also minimized. The least squares equation (22) is written as:

$$\int_{\mathfrak{R}} d^3r' (\mathbb{M}\vec{v}^h)^H \mathbb{M}\vec{\phi}^h + \lambda \left[\int_{\Gamma_1} d\sigma (C_1^T \vec{v}^h)^H C_1^T \vec{\phi}^h + \int_{\Gamma_2} d\sigma (C_2^T \vec{v}^h)^H C_2^T \vec{\phi}^h \right] = \int_{\mathfrak{R}} d^3r' (\mathbb{M}\vec{v}^h)^H \vec{Q} + \lambda \int_{\Gamma_1} d\sigma (C_1^T \vec{v}^h)^H \vec{d} \quad (23)$$

where $\int_{\Gamma} d\sigma$ is the surface integration on the boundaries and λ is a penalization parameter depending on the problem. When λ tends to infinity, the solution is exact on the boundaries.

This approach is general and has been developed as an extension to the Ressel variational functional.^[8] Lately, Manteuffel et al.^[11] have proposed a boundary functional for fixed incoming flux conditions, which allows the demonstration of uniqueness and provides error bounds of the transport equation solution. This functional is written as:

$$\langle \mathcal{L}u, \mathcal{L}\psi \rangle + 2 \int_{\Gamma_1} d\sigma \int_{\vec{n} \cdot \vec{\Omega} < 0} d^2\Omega' \psi u |\vec{n} \cdot \vec{\Omega}| = \langle \mathcal{L}u, q \rangle + 2 \int_{\Gamma_1} d\sigma \int_{\vec{n} \cdot \vec{\Omega} < 0} d^2\Omega' h u |\vec{n} \cdot \vec{\Omega}| \quad (24)$$

This definition shows some resemblances with our penalization technique with $\lambda = 2$ and both methods preserve the symmetry of the system. The preliminary tests of this functional in ARTEMIS show no significant improvements comparing to results with the functional (23). More comparisons are planned in the near future.

The variational functional (23) is well-suited for using continuous finite element interpolation technique. The flux moments are decomposed in finite element approach as:

$$\phi_{lm}^k(\vec{r}) = \sum_{i=1}^{NI} \phi_{lm}^{k,i} \eta^{k,i}(\vec{r}) \quad \forall l = 0, N, \quad -l \leq m \leq l \quad (25)$$

where $\eta^{k,i}$ is the hat function at node i of element k , with NI the number of vertices. One-dimensional and three-dimensional elements are defined for first order interpolation functions, so 2 vertices per element are needed in 1D and 8 vertex for 3D hexaedrons.

The domain \mathfrak{R} is split into M elements. On each element, the functional is computed and the resulting elementary matrices are summed to form the global system. The P_N transport equation is written for a vector of interpolation functions $\vec{\eta}$ as:

$$\mathbb{M}\vec{\eta} = \begin{bmatrix} \mathbf{D}_x & i\mathbf{D}_y & \mathbf{D}_z \end{bmatrix} \begin{bmatrix} \frac{\partial}{\partial x} \vec{\eta} \\ \frac{\partial}{\partial y} \vec{\eta} \\ \frac{\partial}{\partial z} \vec{\eta} \end{bmatrix} + \mathbf{R}\vec{\eta}$$

where $\vec{\eta}$ is composed of $(N + 1)^2$ functions η for each vertex. Note that the complex arithmetics arises only for the streaming matrices \mathbf{D}_x , \mathbf{D}_y and \mathbf{D}_z . The least squares functional (22) is developed to identify standard finite element elementary matrices, stiffness and mass matrices, such as:

$$[K]_{in,jm} = \int_k d^3r \frac{\partial}{\partial x_n} \eta_i \frac{\partial}{\partial x_m} \eta_j; \quad [DN]_{in,j} = \int_k d^3r \frac{\partial}{\partial x_n} \eta_i \eta_j; \quad [M]_{i,j} = \int_k d^3r \eta_i \eta_j$$

where i and j represent vertex indices and x_n and x_m two coordinates from x, y or z . The boundary conditions are integrated over the outside element surfaces.

Using the finite element decomposition of the flux moments (25), equation (23) becomes a linear system, which global matrix is hermitian. The total number of unknowns is the number of flux moments times the number of vertices. They are ordered from the first vertex with all its moments to the last vertex.

Then the global matrix is a block-matrix where the contributions of flux moments to one another are kept in block of $(N + 1)^2 \times (N + 1)^2$.

The global matrix is sparse due to the finite element method and to the P_N approximation. Different storage methods were explored element-by-element or Compressed-Sparse-Row (CSR) by block. Here two CSR storage are used, one for vertex interaction and the other for each moment block. A preconditioned conjugate gradient method^[13] has been used to solve the linear system. This allows for the modification of matrix storage without modifying the solver. A specific block symmetric successive relaxation preconditioner is also defined to accelerate convergence.

4. NUMERICAL RESULTS

The ARTEMIS code is written in Fortran-90 and uses the formalism of free-format input decks, allowing easy description of different test cases. Isotropic, anisotropic and multi-group tests were performed to assess the ARTEMIS approach for one-dimensional problems as well as three-dimensional geometries.^[8] Results are well compared to the theoretical basis of the least-squares method. To illustrate the anisotropic extension and void treatment, two problems are here proposed: a one-dimensional case with multigroup anisotropic media and a three-dimensional benchmark with void regions. All the geometric dimensions are given in cm and all cross sections are in cm^{-1} .

First, an anisotropic P_3 scattering test case from Riyait and Ackroyd^[14] was investigated. It is a two-region two-group source problem, which properties are given in Table I. The geometry is a slab of

Table I: Cross sections for the P_3 scattering problem.

Group	$g \rightarrow g$						$g \rightarrow g + 1$			
g	q	σ	σ_0	σ_1	σ_2	σ_3	σ_0	σ_1	σ_2	σ_3
1	1.0	1.0	1/2	3/10	1/5	3/35	1/2	3/10	1/5	3/35
2	1.0	1.0	1/2	3/10	1/5	3/35	-	-	-	-

$[0, 20]$ with a source region in $[0, 2]$ and homogeneous properties elsewhere. Boundary conditions are reflective in $x = 0$ and vacuum in $x = 20$. ARTEMIS calculations are performed for a P_7 expansion and 90 meshes. The number of mesh is a bit larger than the results presented for FELTRAN^[14] in order to compensate for approximated boundary conditions. In Figure 1 the scalar fluxes in both groups are shown, the attenuation reaches 10^{-7} , which is difficult to reproduce with few flux moments. Results are close to the referenced values,^[14] obtained by an ANISN S_{16} calculation on 320 meshes.

The first Kobayashi benchmark problem^[15] is used to illustrate the direct treatment of void regions in ARTEMIS in 3-D geometries. The geometry of the problem is a cubic source inside a cubic void region inside a transport region, as shown in Figure 2. Details are available in Kobayashi.^[15] The void cross section was exactly set to 0.0 and both cases, pure absorber and 50% scattering, were reproduced.

To show the ray-effect remedies in ARTEMIS, two calculations have been made: one with a 3D Cartesian diamond S_N solver developed by G. Samba and one with ARTEMIS. The S_N solver does not treat reflective boundaries so the geometry is unfolded into a complete cube of size $[-100, 100]^3$.

The ARTEMIS storage requirements are very large, so only a P_3 approximation has been chosen. The geometry 2 is split into $20 \times 20 \times 20$ meshes. The S_N discretization is S_4 and $40 \times 40 \times 40$ meshes to match the ARTEMIS values. The resulting scalar fluxes are shown in Figure 3 and 4, where an iso-surface at $\phi = 0.165 \text{ n/cm}^3 \cdot \text{s}$ is shown. The ARTEMIS 1/8 flux is unfolded on the complete geometry.

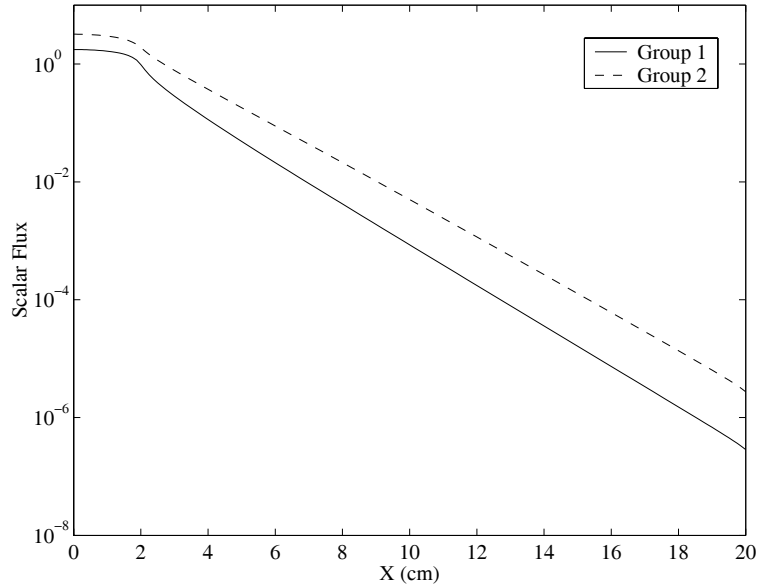


Figure 1: Group fluxes for the anisotropic P_3 scattering test case

In Figure 3, ray effects can be seen as ripples on the iso-surface, but the R_N results are very smooth, following the Cartesian mesh. The spherical harmonics approach warrants a regular solution for the scalar flux, free of ray-effects. However the finite element with a full angular discretization has to be finer to obtain accurate results, which is not feasible with the actual sequential computer code used.

CONCLUSIONS

The least-squares formulation of the transport equation was extended for anisotropic media in the multi-group formalism. Reflective and fixed incoming flux boundary conditions can be applied in 3D Cartesian geometries. The method was encoded into a general sequential code, called ARTEMIS, and numerical results for 1D and 3D problems show that this approach is consistent for obtaining accurate results even in void regions. The finite element discretization leads to very large systems and the approach is still limited to benchmark calculations with coarse meshing. In the coming months, more efficient storage will be investigated and parallel algorithms (multigrid combined with automated domain decomposition) will be used to further extend the application domain of ARTEMIS.

ACKNOWLEDGEMENTS

This work is based in part on a dissertation submitted by the first author (E.V.) for the PhD degree at Ecole Centrale, Paris. Both Commissariat à l'Énergie Atomique (France) and Institut de Génie Nucléaire from Montréal have supported this work.

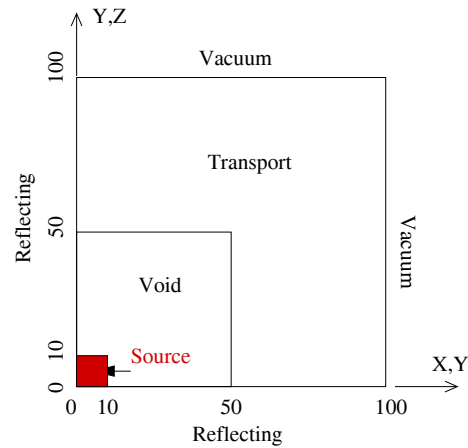


Figure 2: Planar geometry of the first Kobayashi problem

REFERENCES

- [1] R. E. Alcouffe, E. W. Larsen, W. F. Miller, Jr, and B. R. Wienke, “Computational Efficiency of Numerical Methods for the Multigroup, Discrete-Ordinates Neutron Transport Equations: The Slab Geometry Case”, *Nucl. Sci. Eng.*, **71**, pp. 111-127 (1979).
- [2] T. A. Wareing, J. M. McGhee, J. E. Morel, and S. D. Pautz, “ Discontinuous Finite Element S_N Methods on Three-Dimensional Unstructured Grids ”, *Nucl. Sci. Eng.*, **138**, pp. 256-268 (2001).
- [3] J. K. Fletcher, “ The Solution of the Multigroup Neutron Transport Equation Using Spherical Harmonics ”, *Nucl. Sci. Eng.*, **84**, pp. 33-46 (1983).
- [4] R. N. Blomquist and E. E. Lewis, “ A Rigorous Treatment of Transverse Buckling Effects in Two-Dimensional Neutron Transport Computations “, *Nucl. Sci. Eng.*, **73**, pp. 125-139 (1980).
- [5] C. R. E. De Oliveira, “ An Arbitrary Geometry Finite Element Method for Multigroup Neutron Transport with Anisotropic Scattering”, *Progress in Nucl. Energy*, **18**, pp. 227-236 (1986).
- [6] R. T. Ackroyd, “ A Finite Element Method for Neutron Transport- I. some Theoretical Considerations “, *Ann. Nucl. Energy*, **5**, pp. 75–94 (1978).
- [7] K. J. Ressel, “ Least Squares Finite Element Solution of the Neutron Transport Equation in Diffusive Regimes ”, PhD Thesis, University of Colorado at Denver (1994).
- [8] E. Varin, “ Résolution de l’équation de transport neutronique par une méthode de moindres carrés en trois dimensions ”, PhD Thesis, Ecole Centrale Paris, France (2001).
- [9] B. Davison, *Neutron Transport Theory*, Oxford University Press, London (1958).
- [10] G. Arfken, *Mathematical Methods for Physicists*, Academic Press Inc., San Diego (1985).
- [11] T. A. Manteuffel, K. J. Ressel, and G. Starke, “ A Boundary Functional for the Least-Squares Finite-Element Solution of Neutron Transport Problems”, *SIAM J. Numer. Anal.*, **37**, pp. 556-586 (2000).

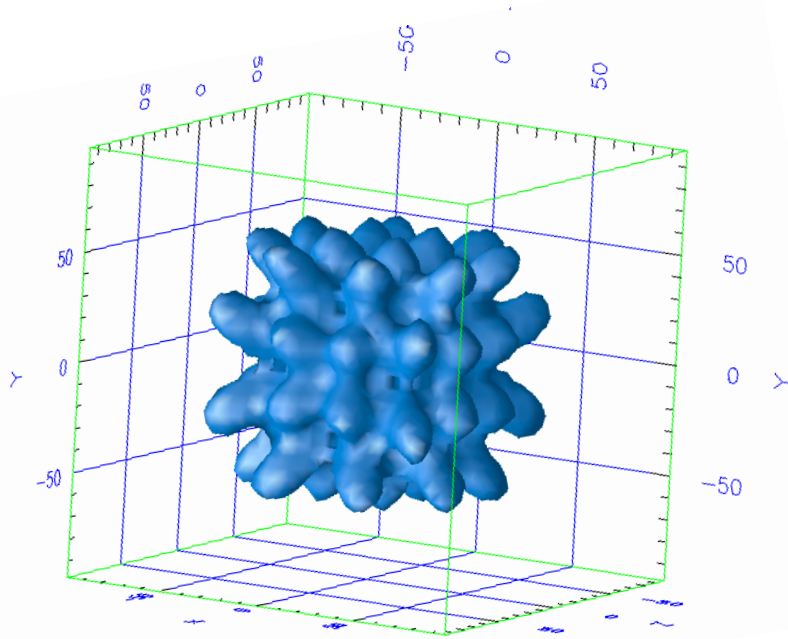


Figure 3: Scalar flux isosurface for Kobayashi Benchmark, 50% scattering case - S_N results

- [12] E. W. Larsen, J. E. Morel and W. F. Miller Jr., "Asymptotic Solutions of Numerical Transport Problems in Optically Thick, Diffusive Regimes", *J. Comp. Phys.*, **69**, 283-324 (1987).
- [13] J. A. Meijerink and H. A. van der Vorst, "An Iterative Solution Method for Linear Systems of which the Coefficient Matrix is a Symmetric M-matrix", *Math. Comp.*, **31** (137), pp. 148-162 (1977).
- [14] N. S. Riyait and R. T. Ackroyd, "The Finite Element Method for Multigroup Neutron Transport: Anisotropic Scattering in 1-D Slab Geometry", *Ann. Nucl. Energy*, **14**, no 3, pp. 113-133 (1987).
- [15] K. Kobayashi, "A Proposal for 3-D Radiation Transport Benchmarks for Simple Geometries with Void Region", *3-D Deterministic Radiation Transport Computer Programs*, *OECD Proceedings*, p. 403 (1997).

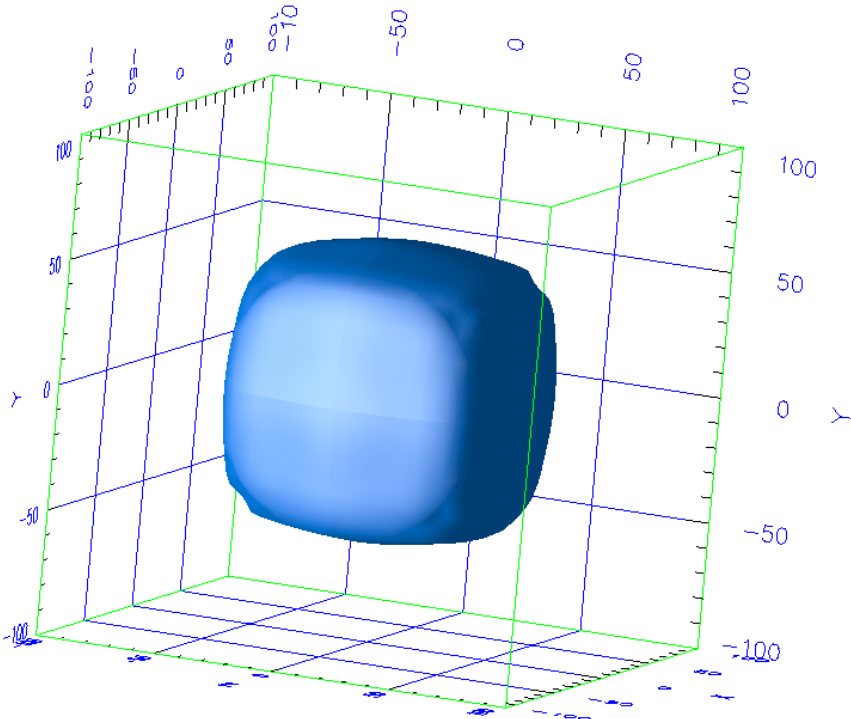


Figure 4: Scalar flux isosurface for Kobayashi benchmark, 50% scattering case - ARTEMIS results